

$p > 2$ spin glasses with first order ferromagnetic transitions

Peter Gillin and David Sherrington

Physics Department, University of Oxford, Theoretical Physics, 1 Keble Road, Oxford. OX1 3NP

Abstract

We consider an infinite-range spherical p -spin glass model with an additional r -spin ferromagnetic interaction, both statically using a replica analysis and dynamically via a generating functional method. For $r > 2$ we find that there are first order transitions to ferromagnetic phases. For $r < p$ there are two ferromagnetic phases, one non-glassy replica symmetric and one exhibiting glassy one-step replica symmetry breaking and aging, whereas for $r \geq p$ only the replica symmetric phase exists.

1 Introduction

The infinite-ranged spherical spin glass with $p > 2$ body random exchange interactions has attracted significant attention recently for a number of reasons. Among these are (i) it is exactly soluble in the thermodynamic limit both for its equilibrium properties and for its off-equilibrium macrodynamics (at least in the sense of coupled equations for macroscopic order functions and *ansätze* solving them in a long time limit), (ii) it exhibits replica symmetry breaking (RSB) and aging glassy macrostates, (iii) the RSB is of the one-step kind (1RSB) even down to the lowest temperatures. (In its discontinuous variant, 1RSB is believed to be symptomatic of many systems exhibiting glassy behaviour without Hamiltonian disorder.)

The original work [1, 2] and most subsequent advances have concentrated on situations where the exchange distribution is symmetric, albeit possibly with an external field. More recently [3] an extension was introduced to allow for an additional ferromagnetic interaction, stimulated by the existence of many physical systems with large coherently coordinated attractors, such as most real spin glass materials with appropriate concentrations [4], neural networks [5], proteins [6], and error-correcting codes [7]. This extension was however limited to two-body ferromagnetic exchange, with corresponding second-order ferromagnetic transitions. In this paper we extend the study further to include $r > 2$ body ferromagnetic interactions for which the onset of ferromagnetism is first order. This is of relevance both for application to real systems (for example, for error-correcting codes $r = p$) and since it brings in new features (spinodal and thermodynamic transitions, metastability, and suppression of glassy ferromagnetism).

2 The model

The Hamiltonian we use is

$$\mathcal{H} = \sum_{i_1 < i_2 \dots < i_p} J_{i_1 \dots i_p} \phi_{i_1} \dots \phi_{i_p} - \frac{J_0(r-1)!}{N^{r-1}} \sum_{i_1 < i_2 \dots < i_r} \phi_{i_1} \dots \phi_{i_r} \quad (1)$$

where the $J_{i_1 \dots i_p}$ are independent quenched random couplings given by a Gaussian distribution with zero mean and variance $p!J^2/2N^{p-1}$. The spins ϕ_i are real numbers subject to the spherical constraint

$$\frac{1}{N} \sum_i \phi_i^2 = 1. \quad (2)$$

We consider $p > 2$ so that replica symmetry is broken for low temperatures, spherical spins so that 1RSB is sufficient at all temperatures, and infinite-ranged interactions so that mean field theory is exact. For $r = 1$ this reduces to the model of [1,2], for $r = 2$ it becomes that of [3], but we shall be interested also in $r > 2$.

In considering the phase diagram, we will identify lines of four types. Since there are first order transitions, in the statics we must consider the spinodal lines (where a phase appears) and the thermodynamic lines (where it becomes thermodynamically preferred due to its free energy). A modified replica analysis employing the criterion of marginal stability (MS) leads to a different set of spinodal lines. Finally, there are spinodal lines generated by a study of the Langevin dynamics at long times. As in the cases studied previously, with an external field [2] or a 2-spin coupling [3], the dynamic lines are identical to the MS lines.

3 Replica theory

The equilibrium properties of this model are given by the replica method [8,9] in which one-step replica symmetry breaking is sufficient. This generates four order parameters governed by self-consistent equations. Three of these describe the probability distribution $P(q)$ of the overlap between pure states: $P(q)$ has two δ -function spikes, one corresponding to the self-overlap

$$q_1 = q^{SS} = \frac{1}{N} \left[\sum_i (\langle \phi_i \rangle^S)^2 \right]_{\text{av}} \quad (3)$$

and one corresponding to the mutual overlap

$$q_0 = q^{SS'} = \frac{1}{N} \left[\sum_i \langle \phi_i \rangle^S \langle \phi_i \rangle^{S'} \right]_{\text{av}}, \quad S \neq S', \quad (4)$$

where $\langle \dots \rangle^S$ refers to the thermodynamic average over the microstates of the pure state S and $[\dots]_{\text{av}}$ to the average over the quenched disorder; the strength of these two are $1-x$ and x respectively. The fourth order parameter is the magnetization M .

The replica free energy F is, in the thermodynamic limit ($N \rightarrow \infty$), given by

$$\frac{2\beta F}{N} = \lim_{n \rightarrow 0} \frac{1}{n} \left[-\frac{\beta^2 J^2}{2} \sum_{ab} q_{ab}^p - \frac{2\beta J_0}{r} \sum_a M_a^r - \ln \det (q - M \otimes M) \right], \quad (5)$$

where the replica indices a and b run from 1 to n , and $M \otimes M$ represents the outer product of the vectors. Under the 1RSB *ansatz* [10] this becomes

$$\frac{2\beta F}{N} = -\frac{\beta^2 J^2}{2} (1 - \overline{q^p}) - \frac{2\beta J_0}{r} M^r - \ln(1 - q_1) - \frac{1}{x} \ln \left(\frac{1 - \overline{q}}{1 - q_1} \right) - \frac{q_0 - M^2}{1 - \overline{q}} \quad (6)$$

where we have defined an average over $P(q)$: for any value of m ,

$$\overline{q^m} = (1-x)q_1^m + xq_0^m. \quad (7)$$

Stationarity of F leads to the self-consistent equations. Extremising with respect to M gives

$$\beta J_0 M^{r-1} = \frac{M}{1 - \overline{q}}; \quad (8)$$

with respect to q_0 and q_1 gives

$$\frac{1}{2} p \beta^2 J^2 q_0^{p-1} = \frac{q_0 - M^2}{(1 - \overline{q})^2}, \quad (9)$$

$$\frac{1}{2} p \beta^2 J^2 (q_1^{p-1} - q_0^{p-1}) = \frac{q_1 - q_0}{(1 - q_1)(1 - \overline{q})}; \quad (10)$$

and with respect to x gives

$$-\frac{1}{2}\beta^2 J^2(q_1^p - q_0^p) + \frac{1}{x^2} \ln \left(\frac{1 - \bar{q}}{1 - q_1} \right) - \frac{q_1 - q_0}{x(1 - \bar{q})} + \frac{(q_0 - M^2)(q_1 - q_0)}{(1 - \bar{q})^2} = 0. \quad (11)$$

For the statics, equations (8), (9), (10) and (11) are solved for M , q_0 , q_1 , and x . We also find it useful to consider the free energy with the magnetization constrained; in this case (8) does not apply. For the calculation under marginal stability, we abandon (11), and instead insist that the lowest eigenvalue of the Hessian matrix of (5) in the q_{ab} should vanish, which is to say that the system should be marginally stable against small fluctuations in the overlaps. The resulting equation is

$$\frac{1}{(1 - q_1)^2} - \frac{1}{2}p(p - 1)\beta^2 J^2 q_1^{p-2} = 0. \quad (12)$$

4 Dynamics

The dynamics used are given by the Langevin equation

$$\frac{\partial \phi_i}{\partial t} = -\beta \frac{\partial \mathcal{H}}{\partial \phi_i} - z(t)\phi_i(t) + \xi_i(t), \quad (13)$$

where $\xi_i(t)$ is a Gaussian thermal noise with zero mean and satisfying

$$\langle \xi_i(t)\xi_j(t') \rangle = 2\delta_{ij}\delta(t - t'), \quad (14)$$

and $z(t)$ is introduced to enforce the spherical constraint (2). The standard generating function procedure [11, 12] yields a self-consistent mean-field equation of motion:

$$\frac{\partial \phi}{\partial t} = \frac{1}{2}p(p - 1)\beta^2 J^2 \int_{-\infty}^t dt' G(t, t') C^{p-2}(t, t') \phi(t') + b(t) - z(t)\phi(t) + \eta(t), \quad (15)$$

where the effective reduced field is $b(t) = \beta J_0 M^{r-1}(t)$, the local response function is $G(t, t') = \delta \langle \phi(t) \rangle / \delta b(t')$, the correlation function is $C(t, t') = \langle \phi(t)\phi(t') \rangle$, the magnetization is $M(t) = \langle \phi(t) \rangle$, and there is a renormalized Gaussian noise $\eta(t)$ with zero mean and satisfying

$$\langle \eta(t)\eta(t') \rangle = 2\delta(t - t') + \frac{1}{2}p\beta^2 J^2 C^{p-1}(t, t'). \quad (16)$$

This equation cannot be solved exactly, but it is possible to obtain self-consistent equations using the standard aging assumption [13]

$$\begin{aligned} C(t, t') &= C_{\text{st}}(t - t') + \mathcal{C}(t'/t), \\ G(t, t') &= G_{\text{st}}(t - t') + \frac{1}{t}\mathcal{G}(t'/t), \end{aligned} \quad (17)$$

taking the limit of long times and setting all the time derivatives to zero. The calculation follows [2] and, as expected, gives the equations (8), (9), (10), and (12) obtained in the MS version of the replica analysis, identifying

$$\begin{aligned} \mathcal{C}(1) &= q_1, & \mathcal{C}(0) &= q_0, \\ C_{\text{st}}(0) &= 1 - q_1, & C_{\text{st}}(\infty) &= 0, \end{aligned} \quad (18)$$

and $M = M(\infty)$. The rôle played by x is that of a factor in a modified fluctuation-dissipation theorem (QFDT) in the non-ergodic phase:

$$\frac{1}{t}\mathcal{G}(t'/t) = -x\beta \Theta(t'/t) \frac{\partial \mathcal{C}(t'/t)}{\partial t'}. \quad (19)$$

There is a direct correspondence between the breaking of replica symmetry and the breaking of ergodicity.

5 Results and interpretation

Phase diagrams for a characteristic set of situations are exhibited in Figures 1–5; the new results are in Figures 3–5 but Figures 1 and 2 are included for orientation (as well as completeness). In each case $p = 4$ is chosen, but similar results apply for other $p \geq 3$. The remaining figures show the free energies of systems with constrained magnetizations: these assist in the interpretation of the phase diagrams which result when the constraint is removed and the free energy minimized with respect to M .

Figure 1 is for $r = 1$ [1, 2], in which case the second term of (1) corresponds to an applied field $h = J_0$. It is helpful to recall its features. For $h > h_c$ the only stable state is paramagnetic. For h between h_c and h_m there is a continuous one-step replica symmetry breaking (C1RSB) transition from paramagnet to spin glass, with $(q_1 - q_0) \rightarrow 0$ at the transition; the transition temperature is the same statically and dynamically, and the transition coincides with the onset of Almeida–Thouless instability. At $h = h_m$, this temperature reaches a maximum of T_m . For $h < h_m$ there is a discontinuous one-step replica symmetry breaking (D1RSB) transition from paramagnet to spin glass, with $x \rightarrow 1$ at the transition. The transition temperature is higher for dynamics (or equivalently marginal stability) than for statics; both transition temperatures are higher than that at which small fluctuation Almeida–Thouless instability would onset were it not preempted by the discontinuous transition. All three temperatures, which we shall label T_d , T_s , and T_{AT} respectively, fall as h falls; for future use we define $T_s = T_s^0$ at $h = 0$. In considering the various systems with ferromagnetic interactions discussed below it will be helpful to make reference to this case.

Before passing to the generalized models it is also useful to consider the system with $J_0 = 0$ (for which case the value of r is irrelevant) but with constrained magnetization. For $T > T_m$ the free energy as a function of M has the form shown in Figure 6(a): the stable state is replica symmetric for all M . As T is reduced below T_m the character of $f(M)$ changes as shown in Figure 6(b), or in more detail in Figure 6(c): a gap opens up in which there is no longer an RS solution stable against Almeida–Thouless fluctuations, and a region in which there is a new RSB solution appears. The RSB solution spans the gap in the RS solution, with an overlap at its lower end. That is, the upper end-point of the RSB curve coincides with the lower end-point of the high- M section of the RS curve, but the lower end-point of the RSB curve lies on the low- M section of the RS curve below its end-point. The RSB solution has monotonically increasing $(q_1 - q_0)$ as M is lowered below the upper connection point of RS and RSB. The coincidence at the upper end of the gap is related to the possibility of a continuous RSB, while the overlap at the lower end is related to a discontinuous RSB. As the temperature is lowered further the gap in the RS curve and range of RSB both grow, with the latter extending to $M = 0$ at $T \leq T_s^0$, as shown in Figure 6(d). For $J_0 = 0$ the minimum of $f(M)$ is always at $M = 0$ which is therefore the unconstrained magnetization. For $T < T_s^0$, where both RS and RSB solutions exist at $M = 0$, the latter is favoured.

Increasing $h = J_0$ for $r = 1$ modifies the curves $f(M)$ and moves the minimum to a finite magnetization $M = M_{\min}$. For $T > T_m$, $f(M)$ remains only RS and the unconstrained state remains paramagnetic. For $T_s^0 < T < T_m$, where there is an RSB curve which does not extend to $M = 0$, the sequence of events on increasing h is as follows: (i) the minimum moves out along the lower section of the RS curve, (ii) it crosses into the region where the RS and RSB curves overlap and both have minima, the RSB being favoured so that a D1RSB transition to a spin glass takes place; (iii) the RSB minimum continues to move out, while the RS minimum reaches the end of the lower RS branch and disappears, corresponding to crossing the Almeida–Thouless line, but the RS minimum is irrelevant and no phase change occurs; (iv) the RSB minimum moves up the RSB curve until this gives way smoothly to the upper section of the RS curve and a C1RSB transition back to a paramagnet takes place. For $T < T_m$ again the RSB curve does extend to $M = 0$ and the system already favours the spin glass solution at $h = 0$, so only (iii) and (iv) occur.

For $r \geq 2$ ferromagnetism becomes possible with effective field

$$h_{\text{eff}} = J_0 M^{r-1} \quad (20)$$

determined self-consistently. Figure 2 shows the phase diagram obtained recently [3] for $r = 2$.

At low J_0 the frustration due to the disorder in J continues to prevent ferromagnetism, as does entropy as the temperature is raised, leading to behaviour similar to that for $J_0 = 0$. At a temperature-dependent J_0 a continuous ferromagnetic transition takes place and the system goes over to a solution whose magnetization rises continuously with J_0 . The ferromagnetic region is split into two parts, non-glassy RS (at higher J_0, T) and glassy 1RSB (at lower J_0, T). The transition between them directly mirrors the behaviour of Figure 1 with h replaced by the self-consistently determined h_{eff} and is D1RSB (C1RSB) for J_0 less (greater) than the value $J_m^{(r)}$ for which $h_{\text{eff}} = h_m$. (The transition temperature reaches the maximum of T_m at $J_0 = J_m^{(r)}$.) Again there is an Almeida–Thouless curve which lies beneath the D1RSB transition line for $J_0 < J_m^{(r)}$ but is coincident with the C1RSB transition line for $J_m^{(r)} < J_0 < J_c^{(r)}$ where $J_c^{(r)}$ is the value of J_0 at which $h_{\text{eff}} = h_c$.

The transitions are apparent in $f(M)$ through behaviour directly analogous to that discussed above for $r = 1$. In the case of $r = 2$ the ferromagnetic onsets are second order, with the minimum in $f(M)$ moving away from $M = 0$ continuously as J_0 is increased across the transition lines. Figure 7 illustrates several aspects of the phase diagram: 7(a) shows a region of non-glassy ferromagnetism above T_m , where $f(M)$ is RS throughout its range; 7(b) shows a non-glassy ferromagnet between T_m and T_s^0 for $J_0 < J_m^{(r)}$, with a gap in the RS curve and an RSB section but with the minimum in the lower RS region; 7(c) shows a glassy ferromagnet at the same temperature, where the minimum is now in the RSB region, the system having undergone a D1RSB transition; 7(d) shows a non-glassy ferromagnet at the same temperature for $J_0 > J_m^{(r)}$, with the minimum now in the upper RS region, the system having undergone a C1RSB transition.

For $r > 2$ the ferromagnetic transitions are first order, with the $M = 0$ solution always locally stable. As noted before, there are two kinds of transition as J_0 is increased or T is decreased: a spinodal transition at which a secondary minimum appears in $f(M)$ at a finite M whilst the lowest minimum is at $M = 0$, and a thermodynamic transition at which the finite M minimum becomes lower than that at $M = 0$. Figures 3–5 show the full phase diagrams for $p = 4$ and $r = 3, 4, 5$ respectively, as characteristic illustrations of systems with first order transitions for which r is less than, equal to, and greater than p . Only for the case $r < p$ is a glassy ferromagnet found with glassy/non-glassy transitions; this transition is analogous to that for the case $r = 2$, with D1RSB for J_0 less than $J_m^{(r)}$ and C1RSB for $J_0 > J_m^{(r)}$. Figure 8 illustrates the underlying character of $f(M)$, which drives the static transitions. Figures 8(a,b) show the situation for $T > T_m$, (a) in a region of spinodal ferromagnetism, (b) of thermodynamic ferromagnetism. Figures 8(c–f) are for $T < T_s^0$, showing the effect of increasing J_0 : (c) is in the spin glass phase, passing to an RSB ferromagnet (d) via a spinodal transition, with the RSB ferromagnet thermodynamically preferable to the spin glass in (e), and eventually crossing via a continuous transition into an RS ferromagnet in (f). The smallest self-consistent value of h_{eff} (i.e. that at the spinodal transition) increases with r , and in fact for $r = p$ at any $T < T_m$ it is exactly that corresponding to the C1RSB line in Figure 1 so that the transition is directly into an RS ferromagnet. This is shown in Figure 9(a). (Note that since the C1RSB line coincides with the Almeida–Thouless line, the RS ferromagnet does become unstable against RSB fluctuations at the transition.) For $r > p$ the smallest h_{eff} is beyond this critical value and carries the system well into the RS region, so there is no trace of an RSB ferromagnet. This is shown in Figure 9(b). Hence for all $r \geq p$ glassy ferromagnetism is suppressed. In the case of $r = p$ the minimum h_{eff} corresponds to the same value of J_0 for any $T < T_m$, yielding a vertical transition line between spin-glass and RS ferromagnet.

For $r > p$ (as in Figure 5) the ferromagnet becomes marginally stable against small fluctuations in M along its spinodal transition line $F_{\text{RS}}''(M) = 0$. The corresponding thermodynamic transition line is in two segments: for $T > T_s^0$ it is given by $F_{\text{FM}} = F_{\text{PM}}$; whilst for $T < T_s^0$ it is where $F_{\text{FM}} = F_{\text{SG}}$. For $r = p$ (as in Figure 4) the spinodal transition is also in two segments: for both segments it has $F_{\text{RS}}''(M) = 0$ as before, but in the lower section ($T < T_m$) it simultaneously becomes unstable against Almeida–Thouless fluctuations. The thermodynamic transition is as for $r > p$. For $r < p$ (as in Figure 3) the spinodal transition line to glassy ferromagnetism is in three segments (see Figure 10): (A) the C1RSB line where $q_1 = q_0$ and $x \neq 1$; (B) the D1RSB line

where $x = 1$ and $q_1 \neq q_0$; (C) the line $F''_{\text{RSB}}(M) = 0$, where it is marginally stable against small fluctuations in M again. Non-glassy ferromagnetism onsets at $F''_{\text{RS}}(M) = 0$, as shown by curve (D) which terminates where it intersects (B). The static and dynamic results are qualitatively the same, although the lines (B) and (C) are slightly displaced. The thermodynamic transition lines are as the spinodal lines for the continuous transitions, but for the first order ferromagnetic transitions are moved to higher J_0 . This curve is in three segments: (C) has moved to the line $F_{\text{SG}} = F_{\text{GFM}}$; the lower section of (B) to $F_{\text{PM}} = F_{\text{GFM}}$; (D) has moved to $F_{\text{PM}} = F_{\text{FM}}$.

6 Conclusions

In this paper we have solved the infinite range spherical p -spin glass with an additional r -spin ferromagnetic interaction, finding the phase diagrams both in statics and dynamics for $p > 2$ and general r . By further examination of the free energy with constrained magnetization we have clarified the origin of the different phases, both for the previously studied models with $r = 1, 2$ and for $r > 2$. We have related the behaviour of systems with $r \geq 2$ to those with $r = 1$. In all cases, in the replica method, the first step of replica symmetry breaking is sufficient. As previously noted [3], for $r = 2$ there are thermodynamically continuous transitions to ferromagnetism with two types of ferromagnetic region, non-glassy and glassy (Figure 2). For $r > 2$ the ferromagnet transitions are first order. For $r < p$ there remains a region of parameter space where the system favours a glassy ferromagnet (Figure 3), whereas for $r \geq p$ glassy ferromagnetism is suppressed and the ferromagnetic region consists of a single non-glassy phase (Figures 4, 5).

Acknowledgments

The authors would like to thank Andrea Cavagna, Irene Giardina, Juan-Pedro Garrahan and John Hertz for helpful discussions. We would also like to thank EPSRC (UK) for financial support, PG for research studentship 97304251 and DS for research grant GR/M04426.

References

- [1] A. Crisanti and H.-J. Sommers, Z. Phys. B **87**, 341 (1992).
- [2] A. Crisanti, H. Horner, and H.-J. Sommers, Z. Phys. B **92**, 257 (1993).
- [3] J. A. Hertz, D. Sherrington, and T. M. Nieuwenhuizen, Phys. Rev. E **60**, 2460 (1998).
- [4] J. A. Mydosh, *Spin glasses: an experimental introduction* (Taylor and Francis, 1993).
- [5] J. A. Hertz, A. Krogh, and R. G. Palmer, *Introduction to the theory of neural computation* (Addison–Wesley, 1991).
- [6] P. G. Wolynes, J. N. Onuchic, and D. Thirumalai, Science **267**, 1619 (1995).
- [7] N. Surlas, Nature **339**, 693 (1989).
- [8] M. Mézard, G. Parisi, and M. A. Virasoro, *Spin Glass Theory and Beyond* (World Scientific, 1987).
- [9] D. Sherrington, “Spin Glasses”, in *Physics of Novel Materials* (World Scientific, 1999), edited by M. P. Das.
- [10] G. Parisi, J. Phys. A **13**, 1101 (1979).
- [11] H. Sompolinsky and A. Zippelius, Phys. Rev. B **25**, 6860 (1982).
- [12] T. R. Kirkpatrick and D. Thirumalai, Phys. Rev. B **36**, 5388 (1987).
- [13] L. F. Cugliandolo and J. Kurchan, Phys. Rev. Lett. **71**, 173 (1993).

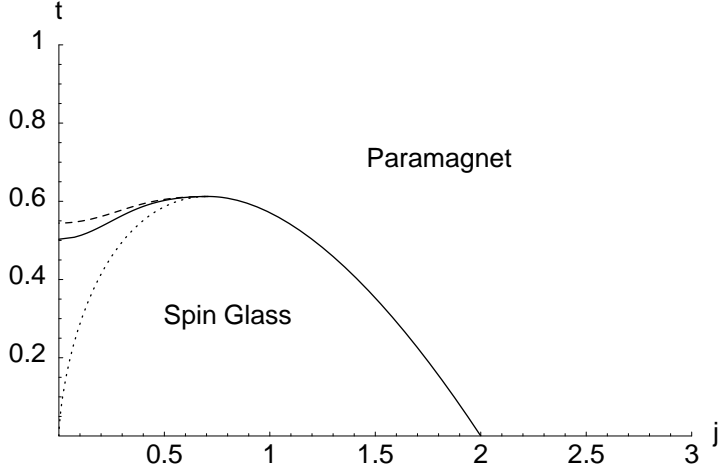


Figure 1: The phase diagram the spin glass with $p = 4$ in a magnetic field h [1,2]. The axes are $j = h/J$ and $t = T/J$. The static result is shown by the solid line; where the dynamic result differs it is shown by the dashed line. The transitions are D1RSB to the left of the maximum and C1RSB to the right. The dotted line is the continuation of the Almeida–Thouless stability line where it does not coincide with the C1RSB. For $p = 4$, the static and dynamic transition temperatures are $T_s^0 \approx 0.503 J$ and $T_d^0 \approx 0.544 J$ at $h = 0$, and both peak at $T = T_m \approx 0.612 J$, $h = h_m = J/\sqrt{2}$ and fall to zero at $h = h_c = 2 J$.

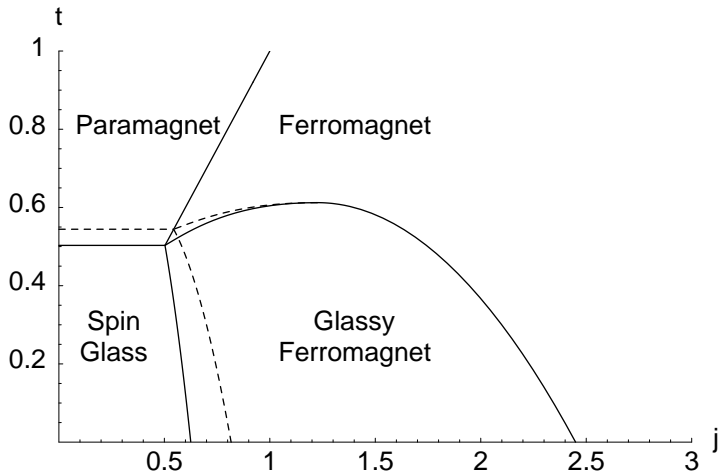


Figure 2: The phase diagram for $p = 4$ and $r = 2$. [3] The axes are $j = J_0/J$ and $t = T/J$. The static results are shown by the solid lines; where the dynamic results differ they are shown by the dashed lines. Transitions to glassy behaviour are D1RSB to the left of the maximum and C1RSB to the right.

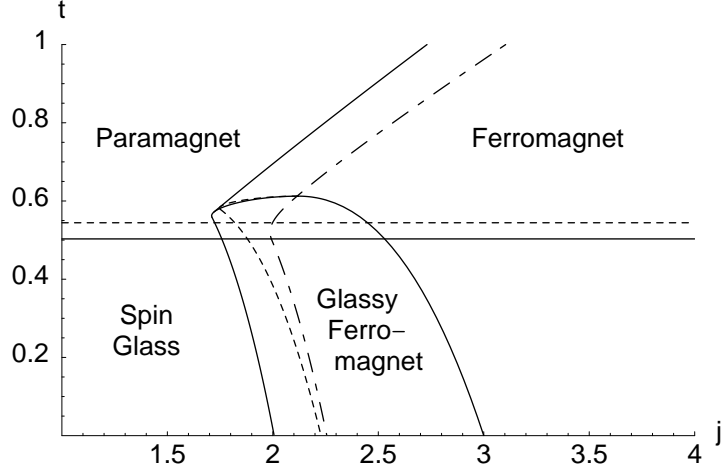


Figure 3: The phase diagram for $p = 4$ and $r = 3$. The axes are $j = J_0/J$ and $t = T/J$. The static spinodal results are shown by the solid lines; where the dynamic results differ they are shown by the dashed line. The dot-dashed line shows the thermodynamic transitions. Transitions to glassy behaviour are D1RSB to the left of the maximum and C1RSB to the right.

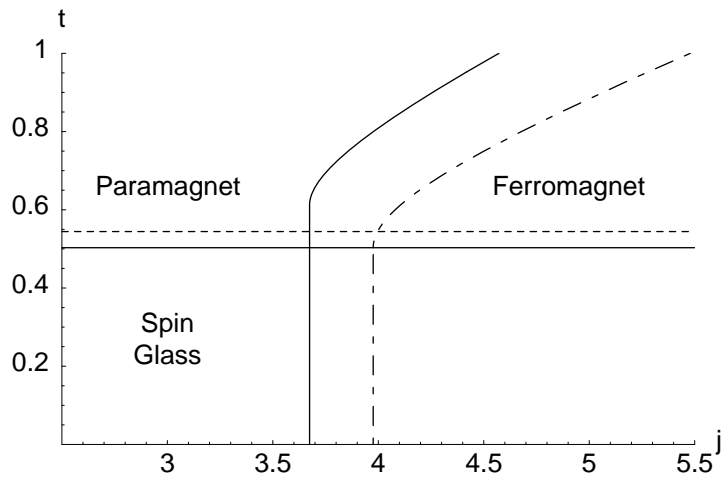


Figure 4: The phase diagram for $p = r = 4$. The axes are $j = J_0/J$ and $t = T/J$. The static spinodal results are shown by the solid lines; where the dynamic results differ they are shown by the dashed line. The dot-dashed line shows the thermodynamic transitions.

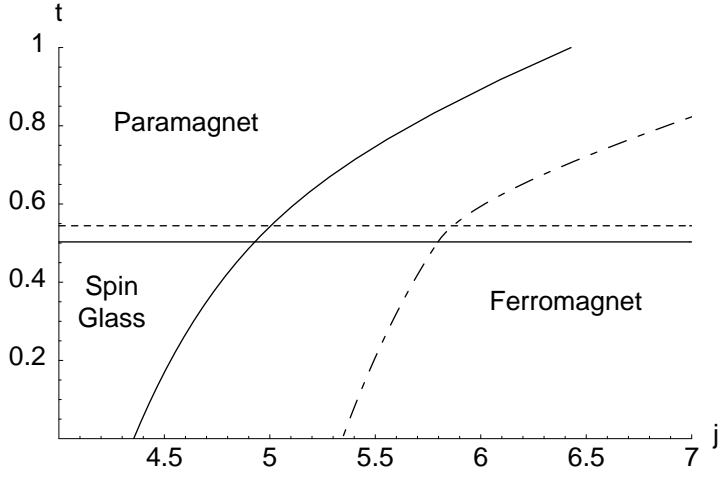


Figure 5: The phase diagram for $p = 4$ and $r = 5$. The axes are $j = J_0/J$ and $t = T/J$. The static spinodal results are shown by the solid lines; where the dynamic results differ they are shown by the dashed line. The dot-dashed line shows the thermodynamic transitions.

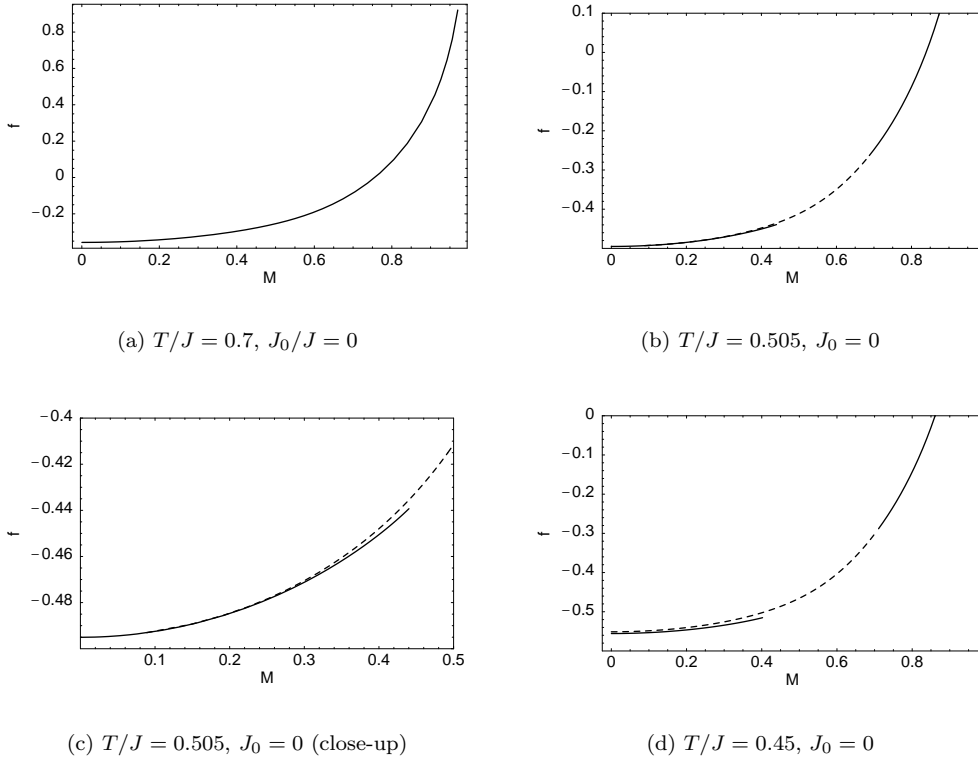
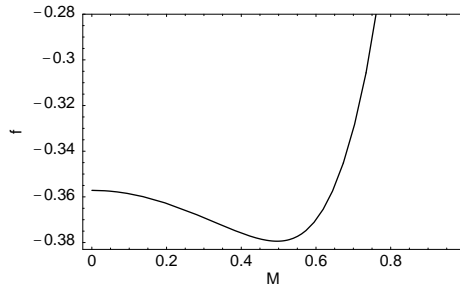
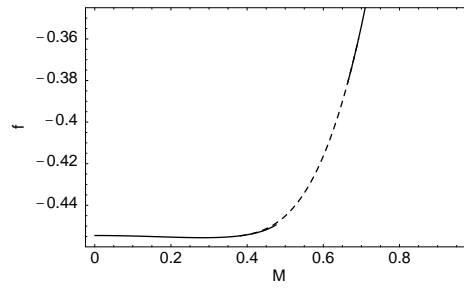


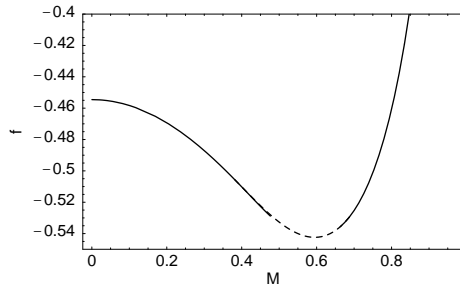
Figure 6: Plots of the free energy per site f against the constrained magnetization M at various temperatures when $J_0 = 0$. (In this case there is no dependence on r .) The solid lines give the RS solutions, the dashed lines the RSB.



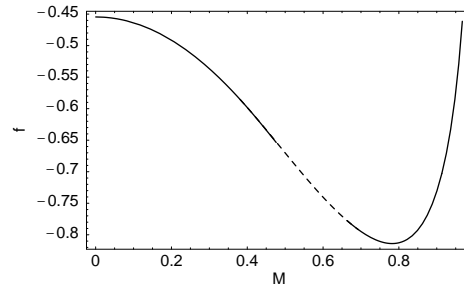
(a) $r = 2, T/J = 0.7, J_0/J = 1$



(b) $r = 2, T/J = 0.55, J_0/J = 0.6$

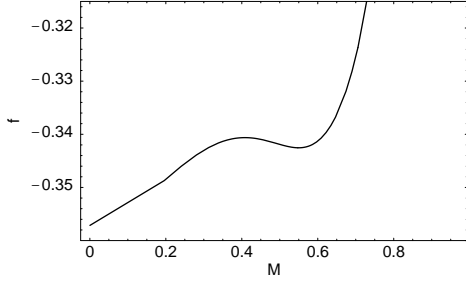


(c) $r = 2, T/J = 0.55, J_0/J = 1.3$

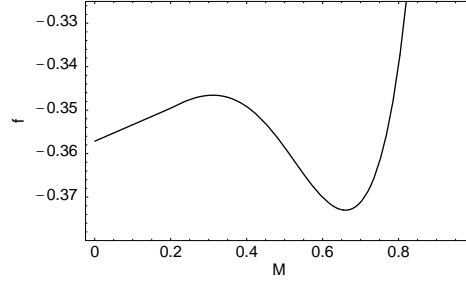


(d) $r = 2, T/J = 0.55, J_0/J = 2.4$

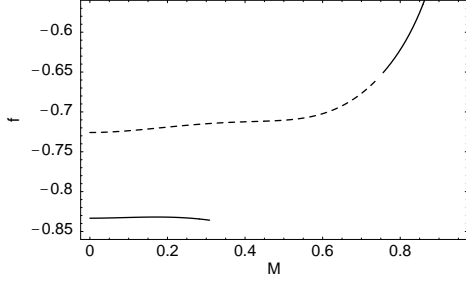
Figure 7: Plots of the free energy per site f against the constrained magnetization M at various points in the phase diagram when $r = 2$. The solid lines give the RS solutions, the dashed lines the RSB.



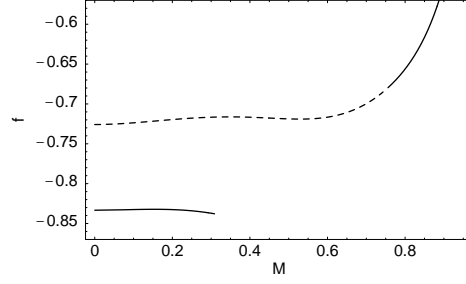
(a) $r = 3, T/J = 0.7, J_0/J = 2.1$



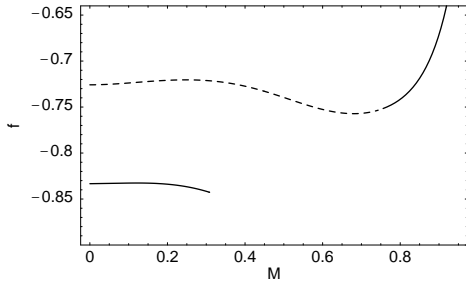
(b) $r = 3, T/J = 0.7, J_0/J = 2.5$



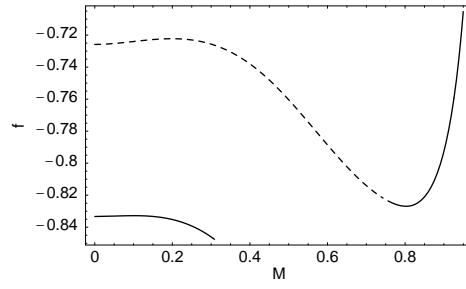
(c) $r = 3, T/J = 0.3, J_0/J = 1.8$



(d) $r = 3, T/J = 0.3, J_0/J = 2$

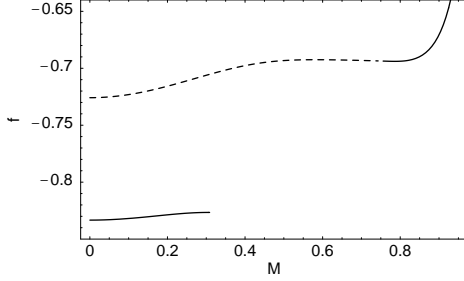


(e) $r = 3, T/J = 0.3, J_0/J = 2.5$

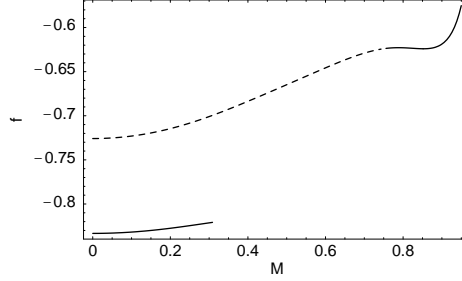


(f) $r = 3, T/J = 0.3, J_0/J = 3$

Figure 8: Plots of the free energy per site f against the constrained magnetization M at various points in the phase diagram when $r = 3$. The solid lines give the RS solutions, the dashed lines the RSB.



(a) $r = 4$, $T/J = 0.3$, $J_0/J = 3.7$



(b) $r = 5$, $T/J = 0.3$, $J_0/J = 4.7$

Figure 9: Plots of the free energy per site f against the constrained magnetization M at a point near the spinodal transition between spin glass and ferromagnet for $r = 4$ and $r = 5$. The solid lines give the RS solutions, the dashed lines the RSB.

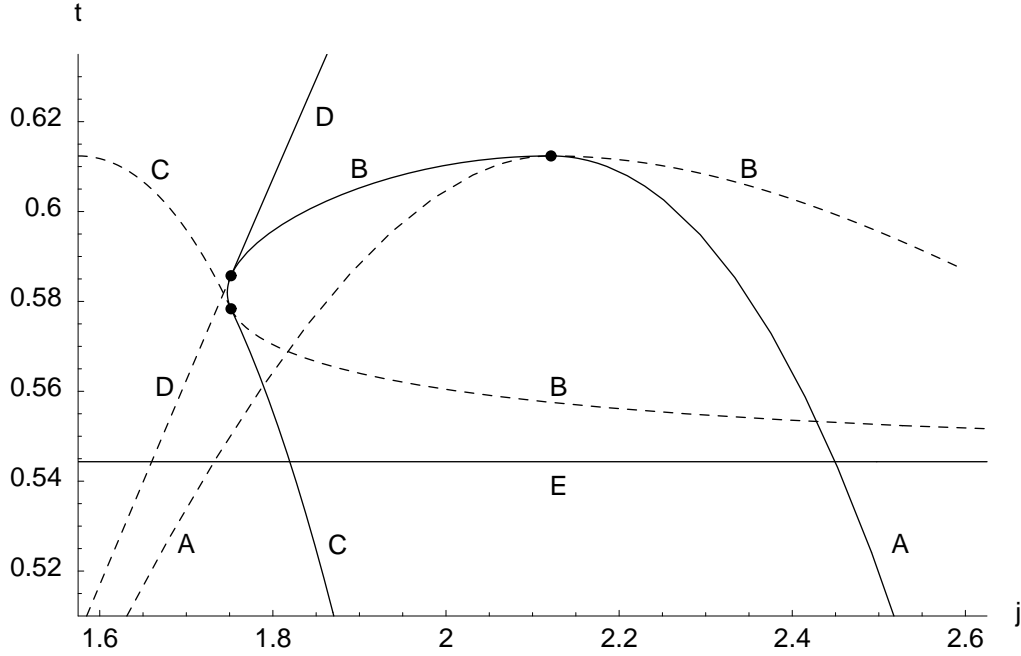


Figure 10: A detail of the dynamic spinodal phase diagram for $p = 4$ and $r = 3$ shown in Figure 3. The axes are $j = J_0/J$ and $t = T/J$. The solid lines are the actual phase transition lines, the dashed lines are their continuations into regions where they are superseded by earlier transitions. For clarity, the points where the various curves meet are marked with dots. A qualitatively similar figure applies for the static spinodal lines. The onset of the glassy ferromagnet is given by 1RSB solutions to (8), (9), (10), and (11), with $M \neq 0$ and the additional constraints $q_1 = q_0$ on (A), $x = 1$ on (B), and $F''_{\text{RSB}}(M) = 0$ on (C). The onset of the non-glassy ferromagnet is given by RS solutions to the equations with $M \neq 0$ and $F''_{\text{RS}}(M) = 0$, and is shown by (D). The onset of the spin glass is given by 1RSB solutions to the equations with $M = 0$ and $x = 1$, and is shown by (E).